Organic & Biomolecular Chemistry

Cite this: *Org. Biomol. Chem.*, 2011, **9**, 4306

www.rsc.org/obc

PAPER

Cytotoxic potency of small macrocyclic knot proteins: Structure–activity and mechanistic studies of native and chemically modified cyclotides†

Robert Burman,[a] Anders Herrmann,[a] Rossetti Tran,[a] Jan-Erik Kivelä,[a] Andrei Lomize,[b] Joachim Gullbo[c] and Ulf Göransson*[a]

Received 1st November 2010, Accepted 11th March 2011
DOI: 10.1039/c0ob00966k

The cyclotides are a family of circular and knotted proteins of natural origin with extreme enzymatic and thermal stability. They have a wide range of biological activities that make them promising tools for pharmaceutical and crop-protection applications. The cyclotides are divided into two subfamilies depending on the presence (Möbius) or absence (bracelet) of a *cis*-Pro peptide bond. In the current work we report a series of experiments to give further insight into the structure–activity relationship of cyclotides in general, and the differences between subfamilies and the role of their hydrophobic surface in particular. Selective chemical modifications of Glu, Arg, Lys and Trp residues was tested for cytotoxic activity: derivatives in which the Trp residue was modified showed low effect, demonstrating the existence of a connection between hydrophobicity and activity. However, over the full set of cyclotides examined, there was no strong correlation between the cytotoxic activity and their hydrophobicity. Instead, it seems more like that the distribution of charged and hydrophobic residues determines the ultimate degree of potency. Furthermore, we found that while the Glu residue is very important in maintaining the activity of the bracelet cyclotide cycloviolacin O2, it is much less important in the Möbius cyclotides. Despite these differences between cyclotide subfamilies, a systematic test of mixtures of cyclotides revealed that they act in an additive way.

Introduction

Cyclotides form a large family of cyclic plant proteins found in the violet (Violaceae) and coffee (Rubiaceae) plant families.[1] They have a remarkable structure featuring three disulfide bonds arranged in a cystine knot—two disulfides and their connecting peptide backbone form an embedded ring that the third disulfide penetrates.[2,3] That knot, together with a head-to-tail cyclic amide backbone defines the cyclic cystine knot (CCK) motif (Fig. 1A and B). The result is a protein scaffold of extraordinary stability,[4] which is able to mediate a range of biological activities. For example, cyclotides have been reported to have anti-fouling,[5] anti-HIV,[6] antimicrobial,[7,8] and insecticidal effects.[9] As such, the CCK motif is now under development into a scaffold for protein engineering for pharmaceutical and agricultural applications.[10,11]

In addition to their considerable biological diversity, the cyclotides also exhibit great structural diversity within the CCK-framework. They are approximately 30 amino acid residues in size and individual plant species express cocktails of more than 50 different cyclotides.[12] To date, around 200 cyclotides have been characterized (see the database of cyclic proteins, Cybase, for the exact number and their sequences),[13,14] but the total number of natural cyclotides is considerably greater than this. It has been suggested that there may be tens of thousands of different cyclotides in Rubiaceae alone.[15]

There are two main cyclotide subfamilies, the Möbius and the bracelet. Möbius cyclotides are distinguished by the presence of a *cis*-Pro peptide bond in loop 5 (the sequence between two adjacent cysteine residues is referred to as a loop; Fig. 1), which is absent in the bracelets. More importantly in the context of the current work, the two subfamilies also differ in terms of their overall net charge and in the distribution of surface-exposed hydrophobic amino acid residues. These differences between the subfamilies are illustrated in detail in Fig. 1A and B, which shows the polar and hydrophobic regions of the prototypic Möbius cyclotide varv A and the bracelet cycloviolacin O2 (cyO2).

The cyclotides' diverse biological activities probably arise from a common mechanism of action, namely their ability to interact with and disrupt lipid membranes. This hypothesis is supported by the results of recent studies on the binding and the mode of binding of cyclotides to lipid membranes,[16,17] and by the results of functional experiments using model lipid membranes and real

[a]*Division of Pharmacognosy, Department of Medicinal Chemistry, Uppsala University, BMC, Box 574, SE-751 23, Uppsala, Sweden. E-mail: ulf.goransson@fkog.uu.se; Fax: +46-18-509101; Tel: +46-18-4715031*
[b]*College of Pharmacy, University of Michigan, Ann Arbor, MI, 48109, USA*
[c]*Division of Clinical Pharmacology, Department of Medical Sciences, University Hospital, Uppsala University, SE-751 85, Uppsala, Sweden*
† Electronic supplementary information (ESI) available. See DOI: 10.1039/c0ob00966k

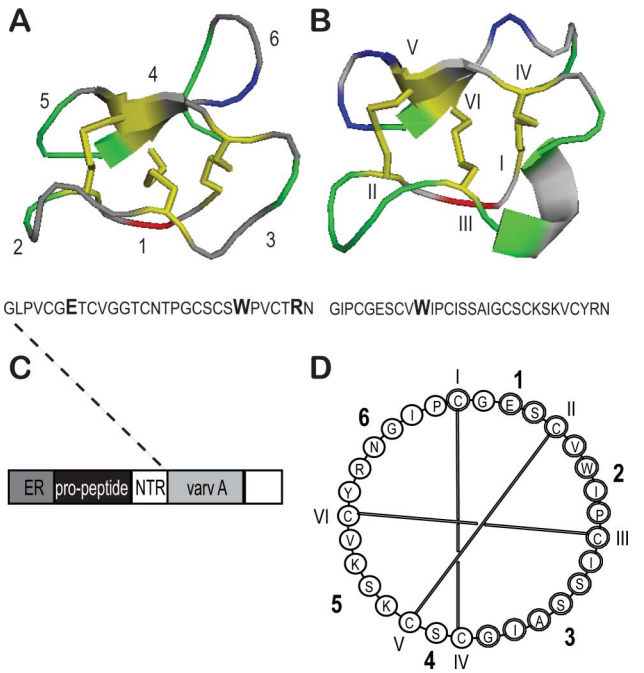

Fig. 1 Schematic representations of the peptide backbone of varv A (A) and cycloviolacin O2 (B). It is convenient to describe the backbone regions of cyclotides between the conserved cysteines as loops 1–6, as shown in (A), whereas individual Cys residues are labeled with Roman numerals I–VI as shown in (B). The cyclic cystine knot (yellow lines), and hydrophobic (green), anionic (red), and cationic (blue) residues. (C) The mRNA encoding the precursor protein of cyclotides are organized as demonstrated by the block diagram. The precursor protein starts with a conserved endoplasmic reticulum region (ER), a pro-peptide region, and an N-terminal repeat region (NTR) followed by the cyclotide region. The NTR and cyclotide region can be repeated 1–3 times in one precursor protein. The sequence of varv A is aligned with the cyclization point (Gly and Asn) at the end of the sequence. (D) shows the disulfide pattern in cycloviolacin O2 with the cysteines connected as Cys I–IV, Cys II–V, and Cys III–VI together with the loop numbers 1–6.

cells.[18,19] However, the precise details of cyclotides' mechanism of action and structure–activity relationships remain unclear.

We have demonstrated that the cyclotides are cytotoxic agents that display strong *in vitro* activity against both cell lines and solid tumor cells in the low micromolar range,[20] but importantly, the bracelet cyclotide cyO2 was shown to be approximately ten times more potent than the Möbius species varv A. On the grounds that one of the main differences between the subfamilies is the presence of a cluster of charged residues in loop 5 of the bracelet cyclotides, it was suggested that electrostatic interactions with the cell membrane might be important determinants of cyclotide activity. We therefore prepared chemically modified derivatives of native cyO2 to examine the importance of the cationic residues Lys, Arg and Glu in determining the cyclotides' activity.[21] Surprisingly, the loss of positive charges did not generally have any significant effect on potency. However, we did find that the lone Glu residue of cyO2 is important in maintaining its activity. By comparing the solution structures (solved by NMR) of the native cyclotide to its Glu-modifed counterpart we determined that the drop in activity is most likely due to a structural change. Methylation prevents Glu from forming a structurally-important set of hydrogen bonds which stabilize the hydrophobic alpha helix in loop 3; this helix might interact with the membrane.[22]

In the current work we describe a series of experiments that were performed to obtain deeper insights into the structure–activity relationships of cyclotides in general and the differences between subfamilies and the role of their hydrophobic surfaces in particular. In our attempts to understand the relationships between structure and cytotoxic activity in the cyclotides, we initially analyzed the activity of native cyclotides, and then targeted a prototypical member of the Möbius subfamily, varv A, and modified its charged residues in the same way as was done previously with the bracelet cyO2.[21] To test the hypothesis outlined above concerning the importance of the hydrophobic surface, we also modified the hydrophobic Trp residue present in both varv A and cyO2. We then used homology modeling to build 3D-structures for all of the cyclotides whose cytotoxic activity has been evaluated to date in order to explore the relationship between their hydrophobic/hydrophilic surface areas and their potency. The orientations of varv A and cyO2 in membranes were subsequently calculated on the basis of these models. Finally, in recognition of the fact that natural cyclotides occur in mixtures and that there is a significant difference in potency between the subfamilies, we evaluated mixtures of pure cyclotides to identify potential sub- or superadditive effects.

Results and discussion

Isolation and chemical modifications of cyclotides

Cyclotides were isolated using a slightly modified version of our previously reported fractionation protocol.[21] MS-MS sequencing was used to confirm the identity of all of the isolated cyclotides. One novel cyclotide, which was named vodo O, was isolated; in this case, the MS-MS sequence was supported by quantitative amino acid analysis. Vodo O was included in the study because of its extreme hydrophobicity, as judged by its late elution during RP-HPLC (Fig. 2). In addition, a derivative of the cyclotide cyO2 in which the Trp residue had been converted to kynurenine was isolated.

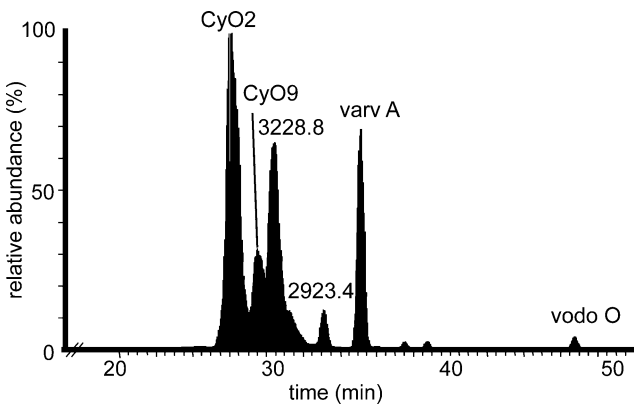

Fig. 2 LC-MS base peak chromatogram (m/z = 800–1800) of the MeOH extract of *Viola odorata* showing the names of the identified cyclotides together with average molecular masses (Da) of unidentified cyclotides. The previously unknown vodo O is the latest-eluting cyclotide in the plant extract; this demonstrates its high hydrophobicity.

The Arg and Glu residues in varv A were modified using the methodology that was previously employed with cyO2.[21] The reaction of the Arg residue with 1,2-cyclohexanedione (CHD) proceeded with a 95% yield, giving the derivative [Arg(CHD)]varvA. Methyl esterification of the Glu residue with acetyl chloride in MeOH gave a 70% yield of the derivative [Glu(Me)]varvA. A varv A derivative with no charged residues was prepared by the sequential application of both of these protocols to give [Glu(Me)]-[Arg(CHD)]varvA.

The Trp residues in cyO2 and varv A were oxidized using N-bromosuccinimide (NBS) in an acetate buffer.[23] In both cases, the native protein was almost completely oxidized after a reaction time of only 1 min at room temperature. Oxidation of varv A gave one early-eluting and highly abundant product with a mass 32 Da greater than that of the native peptide (corresponding to a doubly oxidized product), together with a product with a mass 16 Da greater than that of the parent peptide, corresponding to the singly oxidized product. Oxidation of cyO2 resulted in four products of equal yields, two singly oxidized and two doubly oxidized. The higher number of derivatives for cyO2 is probably due to the microenvironment of the Trp residue: the Trp side chain is more exposed at the molecular surface in cyO2 than in varv A and likely to be more flexible. All major products were tested for cytotoxicity, *i.e.* the double-oxidized varv A and the four oxidized products of cyO2.

As expected, the retention time of the singly-oxidized proteins was only slightly lower than that of the native peptides, but that of the doubly-oxidized species was substantially decreased (Suppl. Fig. 1A and 1B, ESI†). This shows that double and higher oxidation of the Trp residue has a much greater effect on the cyclotides' overall hydrophobicity than does single oxidation. MS-MS sequencing confirmed that the Trp residue was the only residue that has been modified in the oxidized derivatives of varv A and cyO2 (Suppl. Fig. 1C and 1D, ESI†). The UV spectra of the oxidized varv A derivatives were analyzed and showed that the oxidation had occurred on the benzenoid ring and not the C2–C3 double bond of the Trp indole (Fig. 3).

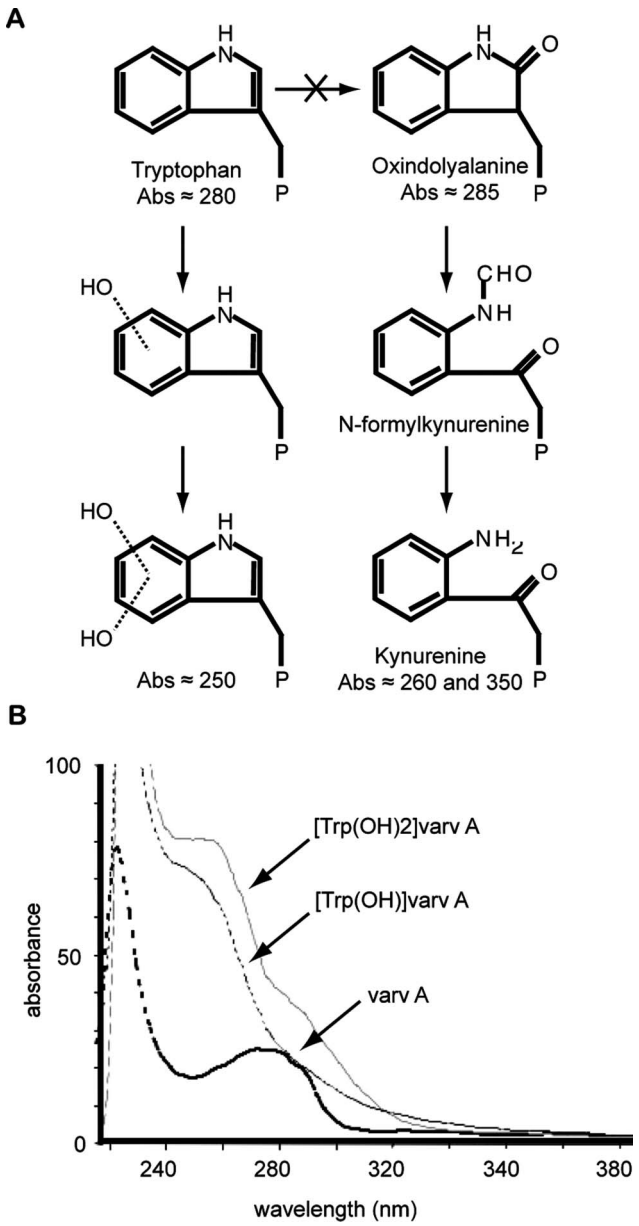

Fig. 3 (A) The left hand side shows some potential alternative oxidation routes, and the absorbance maxima associated with various different products of Trp oxidation. Intermediates in the photo-oxidation of the Trp residue are shown on the right. (B) The arrows indicate absorbance maxima. Varv A (thick black line) has a maximum absorbance band at approximately 280 nm while the spectra of the singly (thin black line) and doubly (grey line) hydroxylated species exhibit absorbance maxima at approximately 250–260 nm. All of the proteins had a common maximum absorbance band at approximately 225 nm (not shown for [Trp(OH)]varvA and [Trp(OH$_2$)]varvA).

Cytotoxic activity of cyclotides

The cytotoxicity of the native cyclotides was tested using the fluorometric microculture cytotoxicity assay (FMCA) with the human lymphoma cell line U-937 GTB; the obtained IC_{50} values are shown in Table 1. The IC_{50} values of the chemically modified derivatives of varv A and cyO2 are shown in Table 2. In all cases, the dose–response curves had very sharp profiles, that is the 10–90% response interval in the log dose–response curves takes place within the narrow concentration range of less than 0.5 μM. This indicates that the different native species and the chemically modified derivatives share a common mechanism of action.

Derivatives of varv A with masked Arg residues did not exhibit reduced activity, but esterification of Glu caused a three-fold reduction in potency. Derivatives of varv A in which both Arg and Glu were modified exhibited a five-fold decrease in potency. Double hydroxylation of the Trp residue in varv A produced a derivative with no cytotoxic activity at 100 μM. In the case of cyO2, the two species in which the benzenoid ring of Trp is monohydroxylated are three times less potent than the native cyclotide, while the doubly-hydroxylated species are almost completely inactive.

Homology modeling and the orientation of cyclotides in membranes

To test the hypothesis that there is a correlation between the hydrophobic surface area of cyclotides and their cytotoxic potency, we created homology models of the assayed cyclotides, using a previously-described technique.[24] As templates, we used the

Table 1 Sequences, cytotoxicities, and structural properties of the bracelet, hybrid, linear and Möbius cyclotides hitherto tested in the FMCA using the human lymphoma cell line U-937 GTB

Protein	Sequence	Net Charge	Surface Area (%) Charged / Hydrophobic	IC_{50} (μM)[3]	Reference
Bracelet					
cyO2[1]	G-IP-CGESCVWIPC-ISSAIGCSCKSKV-CYRN	+2	16.5 / 57.5	0.26–1.8	This study, 20
cyO19[1]	GTLP-CGESCVWIPC-ISSVVGCSCKSKV-CYKD	+1	20.7 / 55.9	0.52±0.7	This study
vitri A	G-IP-CGESCVWIPC-ITSAIGCSCKSKV-CYRN	+2	19.4 / 56.3	0.6	41
psyle E	GVIP-CGESCVFIPC-ISSVLGCSCKNKV-CYRD	+1	21.1 / 58.4	0.76	42
vibi G	GTFP-CGESCVFIPC-LTSAIGCSCKSKV-CYKN	+2	19.4 / 54.3	0.96	26
vibi H	GLLP-CAESCVYIPC-LTTVIGCSCKSKV-CYKN	+2	16.8 / 61.9	1.6	26
vibi E	G-IP-CAESCVWIPCTVTALIGCGCSNKV-CY-N	0	7.2 / 67.7	3.2	26
vodo O	G-IP-CAESCVFIPCTITALLGCGCSNKV-CY-N	0	7.1 / 67.3	3.2±0.3	This study
cyO2(kyn)[1,2]	G-IP-CGESCVWIPC-ISSAIGCSCKSKV-CYRN	+2	—	5.2±0.8	This study
Hybrid					
kalata B8	GSVLNCGETCLLGTC---YTTGCTCNKYRVCTKD	+1	23.7 / 40.7	18±3	This study
psyle A	G-IA-CGESCVFLGC---FIPGCSCKSKV-CYFN	+1	11.7 / 57.5	2	42
Linear					
psyle C	---KLCGETCFKFKC---YTPGCSC-SYPFC-K-	+3	34.2 / 47.5	3.5	42
Möbius					
kalata B2	GL-PVCGETCFGGTC---NTPGCSCTWPI-CTRD	–1	12.8 / 48.5	2.6±0.2	This study
kalata B13	G-LPVCGETCFGGTC---NTPGCACDPWPVCTRD	–2	17.4 / 55.3	3.8±0.5	This study
varv A	GL-PVCGETCVGGTC---NTPGCSCSWPV-CTRN	0	6.0 / 46.0	6.4-10	This study, 20
kalata B1	GL-PVCGETCVGGTC---NTPGCTCSWPV-CTRN	0	5.9 / 45.2	6.9±0.8	This study
varv F	GV-PICGETCTLGTC---YTAGCSCSWPV-CTRN	0	5.8 / 62.9	7.1	20
kalata B7	G-LPVCGETCTLGTC---YTQGCTCSWPI-CKRN	0	16.3 / 48.7	29±10	This study
vibi D	G-LPTCGETCFGGRC---NTPGCTCSYPI-CTRN	+1	15.6 / 39.5	>30	26

[a] cyO2, O19 = cycloviolacin O2, O19 [b] kyn = kynurenine (The tryptophan in loop 2 is naturally modified into a kynurenine) [c] The IC_{50} values from this study are represented with the mean ±SEM

Table 2 Cytotoxic activity and relative potency of native and chemically modified varv A and cycloviolacin O2

Cyclotide derivative	IC_{50} (μM)[a]	Relative potency
varv A		
Native	10 ± 2	1
Arg (CHD)	9.1 ± 2	1
Glu (Me)	34 ± 4	0.33
Arg (CHD) + Glu (Me)	46 ± 7	0.2
Trp $(OH)_2$	>100	<0.1
cycloviolacin O2		
Native	1.8 ± 0.2	1
Trp (OH)	4.5 ± 0.4	0.33
Trp (OH)	5.1 ± 0.5	0.33
Trp $(OH)_2$	55 ± 12	0.03
Trp $(OH)_2$	>100	<0.02

[a] The IC_{50} values represent the mean ± SEM

NMR-structures of the known cyclotides whose sequences were most similar to our targets. The cyclotides' overall surface hydrophobicities were then calculated and are shown in Table 1 together with the sequences and cytotoxic potencies of the modeled peptides.

The results of the orientations of proteins in membranes (OPM)-calculations are shown in Fig. 4 as surface representations whose alignment reflects their calculated orientations in the membrane (represented by the horizontal lines). The different subfamilies have hydrophobic patches at different points on their surfaces, which are reflected in their different membrane-binding orientations. The orientations of both subfamilies have recently been confirmed using NMR.[25] To determine whether the chemical modifications of varv A and cyO2 affected their membrane affinity, the in-membrane orientations of the modified derivatives were also modeled. In keeping with the results of the cytotoxicity assays, the calculated free energies of transfer of cyclotide derivatives with modified Arg and Lys residues from aqueous solution to the lipid bilayer did not differ greatly from those of the native peptides.

The free energies of transfer of the two Glu-modified species were slightly lower than those of the corresponding native peptides, which is seemingly inconsistent with their reduced cytotoxicity. This supports the idea that an explanation for the dramatic loss in potency associated with Glu esterification in cyO2 will require consideration of factors above and beyond the properties of the Glu residue alone.[22] It should however be noted that the OPM experiments do not take into account of interactions other than protein-lipid bilayer, *e.g.* positively charged residues and negatively charged polar phospholipid head groups of the membrane.

Impact of charges on activity

All of the cyclotides that we tested on human lymphoma cells in the FMCA have IC_{50}-values in the low micromolar range, as summarized in Table 1. However the bracelet cyclotides are

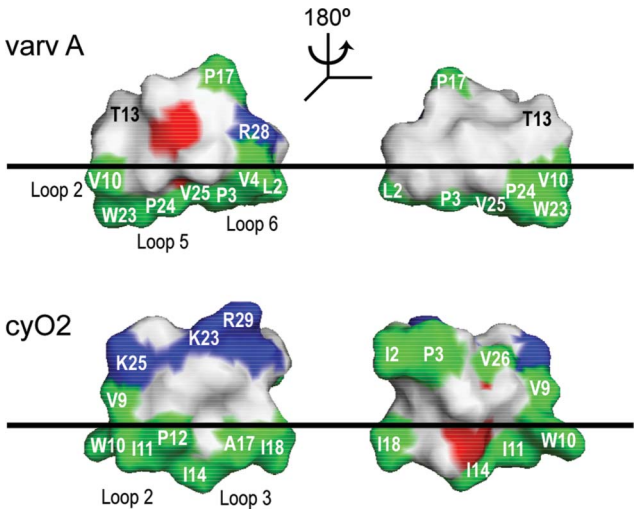

Fig. 4 Orientation of Möbius and bracelet cyclotides in membranes, as calculated using the software program PPM 1.0.[37,38] The plane (line in the picture) represents the hydrocarbon core boundary of the lipid bilayer. The parts of the protein beneath the line are buried in the lipid acyl chain region of the membrane. The parts above the line are located in the lipid head group region (~10 Å thick) and water. The Möbius protein varv A interacts with the lipid bilayer *via* the hydrophobic parts of loops 5 and 6 together with a small part of loop 2. However, loops 2 and 3 of the bracelet cycloviolacin O2 (cyO2) are buried in the membrane. The hydrophobic residues (Ala, Leu, Ile, Pro, Trp, Phe, and Val) are shown in green, cationic residues (Arg and Lys) in blue, anionic residues (Asp and Glu) in red.

clearly more potent than their Möbius counterparts, and within the bracelet subfamily we note that cyclotides containing several cationic residues have slightly higher activity than those of neutral net charge. Interestingly, chemical masking of those additional positively charged residues results in peptides of the same potency as the neutral bracelets (*e.g.* vibi E and vodo O).[26] The trend is not so apparent in the Möbius cyclotides, even though the most potent members of this subfamily, kalata B2 and B13, have extra charged residue(s) in loops 5 and 6. However, these cyclotides also differ from other Möbius cyclotide sequences in other respects; for instance, they have a substitution of Phe for Val/Thr in loop 2. Thus, the presence of charged residues *per se* is not sufficient for potent activity. For comparison the surface representations of varv A, vibi D, cyO2 and vodo O are shown in Fig. 5.

It is commonly suggested that the increased potency of highly charged membranolytic peptides may be due to attractive electrostatic interactions between the peptide and the negatively charged head groups of the phospholipids.[27] However, in the case of cyclotides, a simple sequence comparison reveals that charges in the peptide can also disturb their interactions with the membrane and decrease potency. For example, kalata B7 and vibi D have charged residues in multiple loops; the loss of one cationic residue disturbs the overall amphipathicity of the peptide and thus its activity. When comparing the differences in surface characteristics between prototypical Möbius and bracelet cyclotides, one should note that while both subfamilies are amphipathic, their hydrophilic respective hydrophobic regions are located at different regions.

The hybrid cyclotides kalata B8 and psyle A illustrate the importance of the amphipathic structure. These two cyclotides resemble Möbius cyclotides in all respects but the composition of loop 5. In Möbius species, this loop normally contains

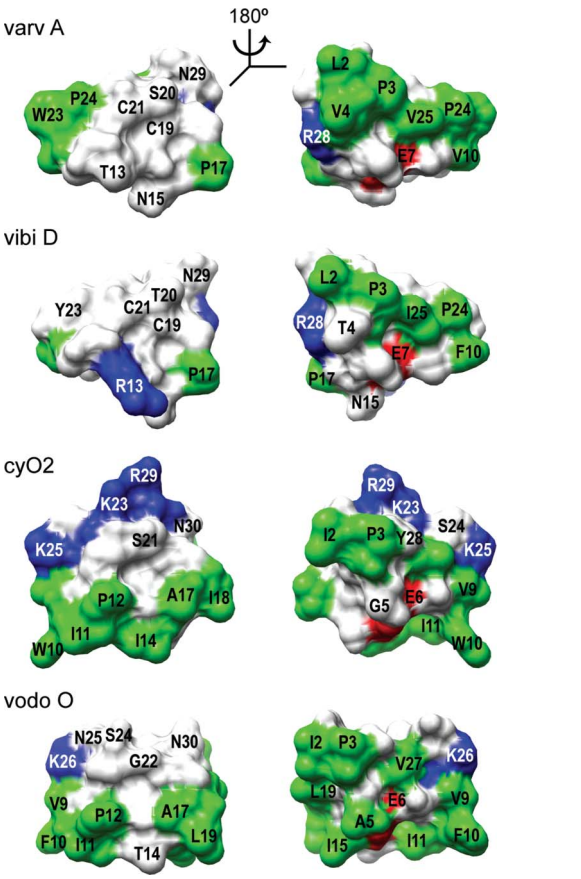

Fig. 5 Surface representations of the bracelet cyclotides cycloviolacin O2 (cyO2) and vodo O, and the Möbius cyclotides varv A and vibi D. The hydrophobic residues (Ala, Leu, Ile, Pro, Trp, Phe, and Val) are shown in green, cationic residues (Arg and Lys) in blue, anionic residues (Asp and Glu) in red.

hydrophobic residues, but in the hybrids, it has been exchanged for a typical bracelet loop containing charged and polar amino acids. This disrupts their amphipathicity and thus reduces their cytotoxicity by a factor greater than 30.

The structural role of the Glu residue and its consequences on activity

Masking the Arg residue in the Möbius cyclotide varv A has no effect on its potency. However, esterification of the Glu residue causes a three-fold loss in potency and the combination of both modifications results in a five-fold decrease. By contrast, in the bracelet cyclotide cyO2, the Glu is the most important charged residue: its esterification causes a 48-fold decrease in potency.[21]

The low potency of [Glu(Me)]cyO2 is probably due to the fact that esterification prevents Glu from participating in hydrogen bonds with the hydrophobic α-helix in loop 3. The loss of these hydrogen bonds significantly affects the conformation of this helix, which becomes more flexible (as shown by NMR studies).[22] While the Glu residue does form hydrogen bonds to loop 3 in the Möbius cyclotides,[3] this loop is significantly less hydrophobic and shorter in this subfamily (NTPG in varv A) and so the esterification of Glu does not have such profound effects on the overall conformation of these peptides.

An intact hydrophobic patch is crucial for activity

The kynurenine derivative of cyO2 makes the protein more hydrophilic (Fig. 3A). This is a naturally occurring derivative resulting from sunlight exposure, as shown by a previous study of kalata B1.[28] Hence, although dried and stored plant material was used for isolation in the current study, it is likely that this derivative also occurs in the living plant. The activity of cyO2(kyn) was significantly lower than that of cyO2, and was comparable to that of singly oxidized species prepared by NBS oxidation (Table 1 and 2). This is the first report of a natural cyclotide degradation product that is less active than the parent peptide.

The effect of decreased hydrophobicity due to oxidation is even more pronounced in synthetic cyO2 derivatives in which the Trp residue is doubly-oxidized, which display no cytotoxicity. Similar losses of activity are observed in oxidized derivatives of varv A, clearly demonstrating the importance of the hydrophobic residues in loop 5 of the Möbius cyclotides. The importance of this residue is further highlighted by the examples of kalata B1, in which the Trp has undergone photo-oxidation, and in synthetic analogs in which Trp has been replaced with some more hydrophilic residue, neither of which possess any hemolytic activity.[28,29]

The importance of the Trp in both cyO2 and varv A can be explained by considering the models shown in Fig. 4. Hydroxylation of the Trp residue would disrupt the hydrophobic patch in both varv A (Trp23) and cyO2 (Trp10). The models demonstrate that when these peptides bind to the membrane, the Trp residue is buried in the lipid bilayer. This probably explains why their potency decreases so dramatically when this residue is hydroxylated. Interestingly, the mono-hydroxylated derivative of cyO2 retained much of the activity of the native species, and it was only when the Trp was doubly oxidized that the peptide lost most or all of its potency. This may be because the hydrophobicity of the other residues that interact with the bilayer is sufficient to keep the monohydroxylated peptide bound in the active orientation and thus to maintain its cytotoxicity.

Cyclotides have additive effects in mixtures

In plants, it has been shown that cyclotides are expressed as cocktails of up to 50 cyclotides,[12] but why plants express so many cyclotides is yet unknown. To identify potential combination effects, cyclotides from both subfamilies were mixed in different ratios and the cytotoxicity of these binary cocktails was analyzed. Three cyclotides were selected for use in a study of the activity of cyclotide mixtures: kalata B1, which is identical to varv A except for a Ser to Thr substitution in loop 4; kalata B2, which was included for the purposes of comparison within the Möbius subfamily; and the bracelet cyclotide cyO2. In order to systematically assess the effects of combining different cyclotides, we compared the IC_{50}-values of individual cyclotides with those of binary cyclotide mixtures having a range of different ratios of the one cyclotide to the other.

Stock solutions of the three cyclotides at concentrations equal to 60 times their IC_{50} values were prepared. The stock solutions were used to prepare series of binary cyclotide mixtures in which the ratio of the concentrations of one stock solution to another varied according to the following sequence: 16 : 1, 8 : 1, 4 : 1, 2 : 1, 1 : 1, 1 : 2, 1 : 4, 1 : 8, and 1 : 16. Dilution series were prepared from these mixtures and their cytotoxicity was evaluated (the assay protocol involved a further and final ten-fold dilution of all samples). A common method for comparing the effects of a combination of bioactive compounds to those of the individual constituents of the combination is to construct an isobologram—a graph of equally effective dose pairs (isoboles) for a single effect level. We chose to look at doses that generate 50% of the maximum observed effect; the doses of the individual cyclotides required to generate this response are plotted as points on the axes of a Cartesian plot.

The straight line connecting the two individual IC_{50} values is the locus of points that will produce this effect if the interaction between the two peptides is additive. This line of additivity makes it possible to quickly compare the experimental result for a given mixture of the two peptides with that expected for an additive interaction; if the experimental result deviates significantly from the line, the two peptides interact in a manner that is either sub- or super-additive.[30]

As shown in Fig. 6, the cyclotide mixtures examined generate results that lie close to the line of additivity, meaning that even mixtures of cyclotides from different subfamilies produce combination effects that are identical to the sum of the individual effects of each component of the mixture. Certain mixtures between cyO2 and kalata B1/kalata B2 at 1 : 1 to 1 : 4 ratios indicate subadditive effects. It is interesting to note that those subadditive effects are observed for mixtures involving cyclotides from both subfamilies, which might indicate for example that binding orientation plays a role for the combined effect or that cyclotide aggregation behaviour influences at certain concentrations. However, a mixture of all three cyclotides (kalata B1, B2 and cyO2) clearly shows that the effect of more complex mixtures is additive (Suppl. Fig. 2, ESI†).

Thus, each cyclotide in the cocktail contributes a small amount to the total effect. However, different cyclotides have different activity profiles against different targets, as has been demonstrated in studies using panels of different assays/targets with a defined set of cyclotides.[7,31] We therefore suggest that plants produce a cocktail of cyclotides with diverse activity profiles such that the cocktail as a whole has excellent potency against as broad a range of targets as possible. Even though one cyclotide may be relatively non-toxic towards human cells, it will contribute to the overall activity of the cocktail and may very well be more active than its siblings against another target. This spread of activity profiles is thus clearly beneficial to the plant.

Conclusion

The results of our chemical modification experiments indicate that the Trp residues in both varv A and cyO2 are important for their biological activity; this is consistent with the results of the OPM calculations, which suggest that the Trp residues are buried in the membrane. These calculations also highlighted a notable difference between the cyclotide subfamilies: bracelet and Möbius cyclotides have very different orientations in membranes. While varv A buries loops 5 and 6 in the membrane, cyO2 interacts with the lipid bilayer through loops 2 and 3. This may explain the different potencies of the two subfamilies. Neither the net charge nor the overall hydrophobicity of the cyclotides correlates strongly with their potency; instead, it seems that it is the distribution of charged and hydrophobic residues that ultimately

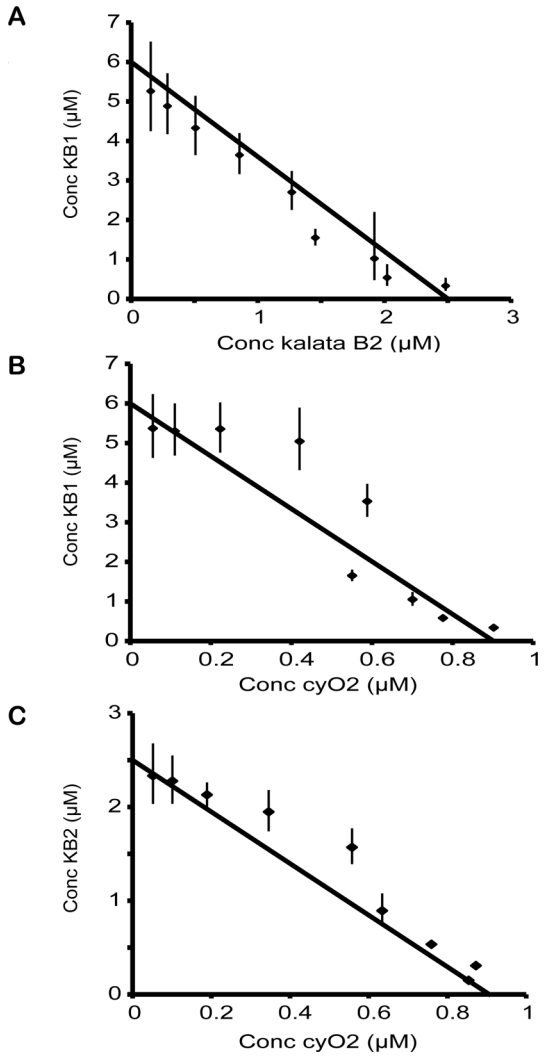

Fig. 6 Isobolograms showing the concentrations of cyclotides mixtures needed to achieve 50% of the maximum observed cytotoxic effect. The diagonal lines mark the line of additivity and the IC_{50} of pure cyclotides (where the line crosses the axes). All data points (nine for each mixture) were close to the line of additivity, meaning that even cyclotides from different subfamilies interact additively – that is to say, their effect in combination is equal to the sum of their individual effects at the same concentrations. KB1 = kalata B1, KB2 = kalata B2 and cyO2 = cycloviolacin O2.

determines a cyclotides' potency, and that the topography of the surface hydrophobicity is the key to its activity. All of the most active cyclotides seemingly have an intact membrane-binding hydrophobic patch, which is the common denominator of their cytotoxic potency. Thus, in order to reliably correlate cyclotides' structures with their potency and to understand their mechanisms of action, it is necessary to consider their structure as a whole rather than focusing exclusively on single residues.

Experimental

Extraction and isolation

CyO2, cyO19, [Trp(kynurenine)]cyO2 and vodo O were isolated from the dried aerial parts of *Viola odorata* L. (Violaceae). Varv A was isolated from *Viola tricolor* L. (Violaceae). Kalata B1, B2, B7, B8 and B13 were isolated from *Oldenlandia affinis* D.C. (Rubiaceae). The cyclotides were extracted and isolated using a previously described method, with some minor differences.[21] Briefly, 100 g of plant material was subjected to two sequential extractions with 4 L of 60% aqueous MeOH. The extract was filtered and subjected to liquid–liquid extraction with dichloromethane (2 : 1). The cyclotides in the aqueous phase were captured on reversed-phase material (C18), eluted with MeOH and then subjected to preparative RP-HPLC. The collected fractions were analyzed using ESI-MS and further purified using HPLC.

High performance liquid chromatography

An ÄKTA basic HPLC system (Amersham Biosciences, Uppsala, Sweden) was used for all HPLC experiments, with detection at 215, 254, and 280 nm. A ReproSil-Pur C18-AQ column (250 × 20 mm i.d., 10 μm, 300 Å) was used for preparative HPLC, with a linear gradient from 10% acetonitrile in 0.05% trifluoroacetic acid (buffer A) to 60% acetonitrile in 0.045% trifluoroacetic acid (buffer B) over 45 min, operated at a flow rate of 5 mL min^{-1}. Native and modified proteins were purified using an ACE C18 column (250 × 10 mm i.d., 5 μm, 300 Å) or a Phenomenex Jupiter C18 column (250 × 10 mm i.d., 5 μm, 300 Å), with a linear gradient increasing from 30% to 70% buffer B over 60 min, operating at a flow rate of 4 mL min^{-1}. A Vydac Everest Analytical C18 column (250 × 4.6 mm i.d., 5 μm, 300 Å) was used to quantify and test the purity of the cyclotides, with a linear gradient from buffer A to buffer B over 40 min, at a flow rate of 1 mL min^{-1}. For LC-MS experiments, a Shimadzu LC-10 system (Shimadzu, Kyoto, Japan) was used with an Everest Narrowbore C18 column (100 × 2.1 mm i.d., 5 μm, 300 Å; Grace Vydac) with a linear gradient from 10% to 60% acetonitrile in 0.1% formic acid operated at a flow rate of 0.3 mL min^{-1}.

Mass spectrometry

For ESI-MS, a Finnigan LCQ ion trap MS (Thermo Electron Co., Waltham, MA, USA) was used in positive ion mode, with the capillary temperature set at 220 °C and the spray voltage at 4 kV. For nanospray MS the samples were dissolved in 50% methanol, 1% formic acid and analyzed with a Protana NanoES source (Proxeon Engineering, Odense, Denmark) mounted on the same instrument, with the capillary temperature set at 150 °C, and spray voltage at 0.5 kV, or with a Q-Tof Micro™ (Waters, Milford, MA) with the voltage set at 1.4 kV. For the latter, the fragmentation spectra were then analysed using MassLynx/BioLynx software (MaxEnt3 and Protein Sequencing).

Chemical modifications

The Glu residue of varv A was esterified by slowly adding 0.2 mL (2.9 mmol, 8300 equivalents) of acetyl chloride to 1 mL of dry MeOH.[32] The mixture was stirred at room temperature for 5 min, and then added to 1 mg (350 nmol) of dry protein. The reaction was allowed to proceed at room temperature for 25 min and quenched by adding 2 mL of water. To modify the Arg residue, 15 mg of 1,2-cyclohexanedione (CHD) (134 mmol, 380 000 equivalents) was dissolved in 5 mL of a 0.2 M solution of aqueous H_3BO_3 containing 1 M NaCl (pH 8.5) and added to 1 mg (350 nmol) of dry protein.[33]

The mixture was allowed to react for 18 h at 37 °C under an atmosphere of N_2 and then quenched by the addition of 2 mL of 30% acetic acid.

The Trp residues of varv A and cyO2 were hydroxylated with N-bromosuccinimide (NBS). A solution of 1 mg mL^{-1} NBS in 80 mM NaAc (pH 5.2) was prepared; 1 mL (56 μmol, 160 equivalents) of this solution was added to 1 mg (350 nmol) of dry protein dissolved in 5 mL of acetate buffer. After 1 min at room temperature, excess L-tryptophan was added to stop the reaction. All reactions were directly purified using HPLC. To test their stability, all of the derivatized peptides were dissolved in 1% DMSO (aq) to a concentration of 100 μM and incubated for 72 h at 37 °C. In all cases, ESI-MS confirmed that no protein degradation had occurred. All proteins tested (native cyclotides and chemical derivatives) in the cytotoxicity assay were >95% pure.

Cyclotide characterization

The amino acid content of the novel cyclotide vodo O was analyzed at the Amino Acid Analysis Center, Department of Biochemistry and Organic Chemistry, Uppsala University. The proteins were hydrolyzed for 24 h at 110 °C with 6 N HCl containing 2 mg mL^{-1} of phenol, and the hydrolysates were analyzed using an LKB model 4151 Alpha Plus amino acid analyzer (LKB Biochrom, Cambridge, UK) using ninhydrin detection.

The sequences of all of the isolated cyclotides and the positions of the modified residues in varv A and cyO2 were confirmed by MS-MS analysis. Before sequencing, the proteins were reduced with dithioerythritol in 0.25 M Tris-containing 1 mM EDTA and 6 M guanidine-HCl (pH 8.5) for 5 h at 37 °C in the dark under an N_2 atmosphere. The free thiols were subsequently S-carbamidomethylated by adding iodoacetamide to the solution. After 1 h at room temperature, the reaction was quenched with citric acid (0.5 M) and the proteins were purified using HPLC. In separate experiments, the S-carbamidomethylated proteins were digested with trypsin, endoproteinase GluC, or chymotrypsin, and finally sequenced using MS-MS.

Native proteins were quantified by weighing (>2 mg cyclotide) or by UV absorbance (<2 mg cyclotide), using a Shimadzu UV-160A spectrophotometer, with calculated molar absorption coefficients of 1880 (vodo O), 3360 (kalata B8), 5940 (varv A, kalata B1, B2, and B13) and 7420 (kalata B7, cyO2 and cyO19) mol^{-1} cm^{-1}, respectively, at 280 nm. The [Trp(kynurenine)]cyO2 was weighed because the calculated absorption coefficient of cyO2 is heavily influenced by the Trp residue, which is modified in this derivative. The chemically modified proteins were quantified using HPLC, integrating at 215 nm, on the basis of two different five-point standard curves constructed by injections of varv A and cyO2, respectively.

Homology modeling and calculation of the orientation of proteins in membranes

Cyclotide homology models were generated using the Modeller 7v7 package from the Departments of Biopharmaceutical Sciences and Pharmaceutical Chemistry, California Institute for Quantitative Biomedical Research, University of California, San Francisco, CA, USA,[34] as described previously.[24] As templates, we used the following structures: kalata B1 (PDB entry 1NB1) for varv A and F; kalata B2 (PDB entry 1PT4) for vibi D; and cyO1 (PDB entry 1NBJ) for vitri A, vodo O, vibi E, G, and H. The templates were selected on the basis of a previously-reported cluster analysis of the cyclotide family.[26]

The MOLMOL software was used to calculate the proportion of the total surface area of each peptide that is hydrophobic (*i.e.* has a surface-exposed Ala, Leu, Ile, Pro, Trp, Phe, Tyr or Val) and the proportion that is charged (*i.e.* has a surface-exposed Arg, Asp, Glu, Gln and Lys). Structures solved by NMR, *i.e.* kalata B1, B2, B8 and cyO2, were obtained from the PDB (entries 1NB1, 1PT4, 2B38 and 2KNM, respectively). Molecular graphics images were produced using the UCSF Chimera package from the Resource for Biocomputing, Visualization, and Informatics at the University of California, San Francisco, CA, USA (supported by NIH P41 RR-01081).[35,36] Orientations of Proteins in Membranes (OPM) calculations were performed as previously described.[37,38]

Preparation of cyclotide mixtures

A stock solution (C_A) of each cyclotide was prepared at a concentration equal to 60× its IC_{50} value. 1 : 1 dilution series were prepared from these stock solutions, diluting with 10% ethanol to give a total of four solutions in total (C_A to C_D). Cyclotide mixtures were then prepared from the dilution series by mixing C_A of one cyclotide with C_A to C_D of another in a 1 : 1 ratio. This was repeated for each C_A so as to cover all possible combinations of C_A solutions with C_A to C_D solutions (21 in total). Dilution series were prepared from these mixed solutions, diluting with 10% ethanol; a final tenfold dilution of the samples was performed in the latter stages of the assay protocol.

Cytotoxicity assay

The cytotoxicity of individual cyclotides and mixtures was determined using the fluorometric microculture cytotoxicity assay (FMCA)[39,40] with the human lymphoma cell line U-937 GTB. The cytotoxic properties of the mixed cyclotide dilution series were determined at three occasions and the individual cyclotides were tested in duplicates at three occasions. The proteins were dissolved in 10% DMSO (aq) or 10% ethanol (yielding a final organic solvent content of 1% by volume in the assay samples) and dilution series were prepared. The assays were performed using V-shaped, 96-well microtiter plates (Nunc, Roskilde, Denmark). Each plate contained six blank wells (200 μl per well of cell-growth medium) and six solvent-control wells (20 μL per well of 10% DMSO or 10% ethanol); 20 μL of protein test solution was added to each of the remaining wells. A suspension of tumor cells in cell-growth medium was dispensed into the sample and solvent control wells (20 000 cells/180 μL per well), which were then incubated for 72 h at 37 °C under 5% CO_2, followed by 40 min incubation with fluorescein diacetate (which is converted to fluorescein by cells with intact plasma membranes).

The fluorescence in each well was measured with a Fluoroscan II at 538 nm, following excitation at 485 nm. The fluorescence is proportional to the number of living cells and cell survival is quantified as a survival index (SI) expressed in percent. The SI is defined as the fluorescence of the test wells relative to the average fluorescence of the control wells (PBS), minus the average fluorescence of the blank wells subtracted. IC_{50} values,

which correspond to the concentration that gave an SI of 50%, were calculated using non-linear regression in GraphPad Prism 4 (GraphPad Software, Inc., San Diego, CA, USA).

Acknowledgements

UG is supported by grants from the Swedish Research Council (#621-2007-5167) and the Swedish Foundation for Strategic Research (#F06-0058). AL was supported by grant 0849713 from the National Science Foundation.

Notes and references

1 D. J. Craik, N. L. Daly, T. Bond and C. Waine, *J. Mol. Biol.*, 1999, **294**, 1327–1336.
2 U. Göransson and D. J. Craik, *J. Biol. Chem.*, 2003, **278**, 48188–48196.
3 K. J. Rosengren, N. L. Daly, M. R. Plan, C. Waine and D. J. Craik, *J. Biol. Chem.*, 2003, **278**, 8606–8616.
4 M. L. Colgrave and D. J. Craik, *Biochemistry*, 2004, **43**, 5965–5975.
5 U. Göransson, M. Sjögren, E. Svangård, P. Claeson and L. Bohlin, *J. Nat. Prod.*, 2004, **67**, 1287–1290.
6 K. R. Gustafson, T. C. McKee and H. R. Bokesch, *Curr. Protein Pept. Sci.*, 2004, **5**, 331–340.
7 J. P. Tam, Y. A. Lu, J. L. Yang and K. W. Chiu, *Proc. Natl. Acad. Sci. U. S. A.*, 1999, **96**, 8913–8918.
8 M. Pränting, C. Lööv, R. Burman, U. Göransson and D. I. Andersson, *J. Antimicrob. Chemother.*, 2010, **65**, 1964–1971.
9 C. Jennings, J. West, C. Waine, D. Craik and M. Anderson, *Proc. Natl. Acad. Sci. U. S. A.*, 2001, **98**, 10614–10619.
10 D. J. Craik, M. Cemazar and N. L. Daly, *Curr Opin Drug Discov Devel*, 2007, **10**, 176–184.
11 P. Thongyoo, C. Bonomelli, R. J. Leatherbarrow and E. W. Tate, *J. Med. Chem.*, 2009, **52**, 6197–6200.
12 M. Trabi and D. J. Craik, *Plant Cell*, 2004, **16**, 2204–2216.
13 C. K. Wang, Q. Kaas, L. Chiche and D. J. Craik, *Nucleic Acids Res.*, 2008, **36**, D206–210.
14 J. P. Mulvenna, C. Wang and D. J. Craik, *Nucleic Acids Res.*, 2006, **34**, D192–194.
15 C. W. Gruber, A. G. Elliott, D. C. Ireland, P. G. Delprete, S. Dessein, U. Göransson, M. Trabi, C. K. Wang, A. B. Kinghorn, E. Robbrecht and D. J. Craik, *Plant Cell*, 2008, **20**, 2471–2483.
16 Z. O. Shenkarev, K. D. Nadezhdin, V. A. Sobol, A. G. Sobol, L. Skjeldal and A. S. Arseniev, *FEBS J.*, 2006, **273**, 2658–2672.
17 H. Kamimori, K. Hall, D. J. Craik and M. I. Aguilar, *Anal. Biochem.*, 2005, **337**, 149–153.
18 Y. H. Huang, M. L. Colgrave, N. L. Daly, A. Keleshian, B. Martinac and D. J. Craik, *J. Biol. Chem.*, 2009, **284**, 20699–20707.
19 E. Svangård, R. Burman, S. Gunasekera, H. Lövborg, J. Gullbo and U. Göransson, *J. Nat. Prod.*, 2007, **70**, 643–647.
20 P. Lindholm, U. Göransson, S. Johansson, P. Claeson, J. Gullbo, R. Larsson, L. Bohlin and A. Backlund, *Cancer Biol. Ther.*, 2002, **1**, 365–369.
21 A. Herrmann, E. Svangård, P. Claeson, J. Gullbo, L. Bohlin and U. Göransson, *Cell. Mol. Life Sci.*, 2006, **63**, 235–245.
22 U. Göransson, A. Herrmann, R. Burman, L. M. Haugaard-Jonsson and K. J. Rosengren, *ChemBioChem*, 2009, **10**, 2354–2360.
23 T. F. Spande, M. Wilchek and B. Witkop, *J. Am. Chem. Soc.*, 1968, **90**, 3256–3258.
24 E. Svangård, U. Göransson, D. Smith, C. Verma, A. Backlund, L. Bohlin and P. Claeson, *Phytochemistry*, 2003, **64**, 135–142.
25 C. K. Wang, M. L. Colgrave, D. C. Ireland, Q. Kaas and D. J. Craik, *Biophys. J.*, 2009, **97**, 1471–1481.
26 A. Herrmann, R. Burman, J. S. Mylne, G. Karlsson, J. Gullbo, D. J. Craik, R. J. Clark and U. Göransson, *Phytochemistry*, 2008, **69**, 939–952.
27 A. Strömstedt, L. Ringstad, A. Schmiidtchen and M. Malmsten, *Curr. Opin. Colloid Interface Sci.*, 2010, **15**, 467–478.
28 M. R. Plan, U. Göransson, R. J. Clark, N. L. Daly, M. L. Colgrave and D. J. Craik, *ChemBioChem*, 2007, **8**, 1001–1011.
29 R. J. Clark, N. L. Daly and D. J. Craik, *Biochem. J.*, 2006, **394**, 85–93.
30 R. J. Tallarida, *J Pharmacol Exp Ther*, 2001, **298**, 865–872.
31 D. C. Ireland, C. K. Wang, J. A. Wilson, K. R. Gustafson and D. J. Craik, *Biopolymers*, 2008, **90**, 51–60.
32 D. F. Hunt, J. R. Yates 3rd, J. Shabanowitz, S. Winston and C. R. Hauer, *Proc. Natl. Acad. Sci. U. S. A.*, 1986, **83**, 6233–6237.
33 J. Pedreno, J. L. Sanchez-Quesada, A. Cabre and L. Masana, *Thromb. Res.*, 2000, **99**, 51–60.
34 M. A. Marti-Renom, A. C. Stuart, A. Fiser, R. Sanchez, F. Melo and A. Sali, *Annu. Rev. Biophys. Biomol. Struct.*, 2000, **29**, 291–325.
35 M. F. Sanner, A. J. Olson and J. C. Spehner, *Biopolymers*, 1996, **38**, 305–320.
36 E. F. Pettersen, T. D. Goddard, C. C. Huang, G. S. Couch, D. M. Greenblatt, E. C. Meng and T. E. Ferrin, *J. Comput. Chem.*, 2004, **25**, 1605–1612.
37 A. L. Lomize, I. D. Pogozheva, M. A. Lomize and H. I. Mosberg, *Protein Sci.*, 2006, **15**, 1318–1333.
38 M. A. Lomize, A. L. Lomize, I. D. Pogozheva and H. I. Mosberg, *Bioinformatics*, 2006, **22**, 623–625.
39 R. Larsson and P. Nygren, *Anticancer Res*, 1989, **9**, 1111–1119.
40 E. Lindhagen, P. Nygren and R. Larsson, *Nat. Protoc.*, 2008, **3**, 1364–1369.
41 E. Svangård, U. Göransson, Z. Hocaoglu, J. Gullbo, R. Larsson, P. Claeson and L. Bohlin, *J. Nat. Prod.*, 2004, **67**, 144–147.
42 S. L. Gerlach, R. Burman, L. Bohlin, D. Mondal and U. Göransson, *J. Nat. Prod.*, 2010, **73**, 1207–1213.

